

**Introduction:** Impact craters which are neither circular nor elliptical and display at least two linear rim segments with a distinguishable angle between them are considered polygonal. Polygonal craters can form any regular polygon, with a hexagon displaying at least two to four distinct linear rim segments being the most common [1]. Previous studies show polygonal craters can form at any crater diameter [1-3] but are mainly found above the simple-to-complex transition diameter ( $D_{sc}$ ) at diameters between  $D_{sc}$  and  $5 D_{sc}$  [1]. The formation of polygonal craters is structurally controlled due to preexisting joint patterns or faults [4]. Since the craters are structurally controlled, they can provide insight into underlying tectonic structures not seen on the body's surface [4]. It has been noted that degradation does not play a significant effect in the polygonality of the crater and the relation between the shape and existence of these craters with respect to the age of the preexisting joint patterns is still not well understood [5].

Investigation of polygonal craters have been conducted throughout the solar system due to their presence on rocky and icy bodies. The polygonal craters found on rocky bodies are generally 10-20% of all known craters on these bodies [6]. Several studies of polygonal craters have been conducted on Ceres to identify the presence of these craters, the number of linear rim segments, and the mean angle between linear rim segments. Of the 76 IAU-approved named craters on Ceres, 74% displayed distinguishable linear rim segments resulting in a mean angle of  $133^\circ$ , similar to the angle found for polygonal craters on Vesta [5]. Further investigation revealed 258 polygonal craters with diameters between 5-280 km with ~120 displaying six linear rim segments [7]. A follow up study of craters between 1 and 280 km revealed 276 polygonal craters [8].

This study utilizes a global crater database created for Ceres to establish a comprehensive method for classifying polygonal craters. This method analyzes several properties of polygonal craters in a larger diameter range than previously reported for Ceres. These data include the number of polygonal craters, their number of linear rim segments, the mean angle for each crater, the orientation of these polygonal craters in relation to surface fractures (either inside or

outside of the crater), and the mean angle for the linear rim segments in relation to the visible fractures.

**Methodology:** We have developed a global Cerean crater database containing 44,594 craters  $\geq 1.0$  km in diameter and have categorized 1,466 craters as polygonal (3% of total) for further study [Figure 1]. Data were attained from the Framing Camera (FC) on NASA's Dawn spacecraft with a resolution of 400m/pixel. The imagery obtained from the Low Altitude Mapping Orbit (LAMO) with a resolution of 35m/pixel [9] was used to further investigate these polygonal craters. A separate database was created containing four categories: a polygonal crater with no visible fractures inside or outside of the crater, a polygonal crater with visible fractures inside of the crater, a polygonal crater with visible fractures outside of the crater, and a polygonal crater with visible fractures inside and outside of the crater. Visible fractures outside of the crater were only considered related to said segments of the crater if the distance from each linear rim segment of the crater was no more than 10 crater radii away. Each of these measurements were taken with the crater in the center of the frame in the due north position.

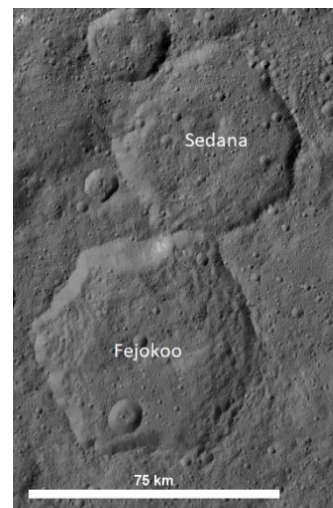


Figure 1. Fejokoo crater ( $D = 68.0$ -km) centered at  $29.15^\circ\text{N } 312.11^\circ\text{E}$ . Sedana crater ( $D = 58.0$ -km) centered at  $36.5^\circ\text{N } 314.7^\circ\text{E}$ .

The analysis includes a comparison of the orientation of the polygonal crater's linear segments with previously mapped linear features across the surface [10]. These features include the Samhain Catena, Uhola Catena, Pongal Catena, Baltay Catena, Gerner Catena, and Junina Catena. Fractures found within a crater were reported in the global crater database used for this analysis.

We utilized the ImageJ software to obtain angle measurements for the angle between linear rim segments and the angles between the linear segments and the fractures. The database contains several columns of information about each polygonal crater including the number of sides (ranging from 4-12), the angle measurements for each linear rim segment to its adjacent segment, the mean angle for the crater, the angle between the linear rim segments and the visible fractures (within the crater or outside of the crater), the mean angle for the crater with fractures, the direction of the fracture in relation to the crater (i.e north, south, east, west), and the name of the fracture associated with the crater, if applicable.

**Preliminary Results:** Table 1 shows the number of the 1,466 polygonal craters which fell into one of the four categories analyzed.

Polygonal Crater Classification	Number of Craters
No Fractures	1225
Fractures Inside of the Crater	3
Fractures Outside the Crater	227
Fractures Inside & Outside	11

Table 1: Number of polygonal craters in the four categories analyzed.

Many craters did not display visible fracture inside of the crater, as well as being out of range of any visible linear features outside of the crater. This was mainly due to the limitation of the 10 crater radii distance which affected how far smaller crater diameters would extend outward.

Craters classified as polygonal fell within all crater diameters and crater degradation states. The smallest polygonal crater was 1.0 km and the largest was 282.0 km (Kerwan). The most frequent number of linear rim segments was six similar to previous studies identifying six sides as being the most frequent [7]. Table 2 shows the number of craters displaying varying numbers of linear rim segments.

The average angle between linear rim segments was 122.7° which is smaller than what has been previously reported [6]. The reason for the difference between measurements is due to the increase in sample size in this study. The mean angle between linear rim segments also varies among the four categories, with polygonal craters unaffected by visible fractures having a mean angle of 122.2° and craters with fractures inside and near linear features outside of the crater being 133.5° which is more

similar to previous studies [6]. The reason the latter shows similar angle measurements to the previous study, which only investigated official named craters, is due to 8 of the 11 craters in this category being official named [6].

Number of Linear Rim Segments	Number of Craters
4 sides	5
5 sides	184
6 sides	629
7 sides	367
8 sides	196
9 sides	58
10 sides	18
11 sides	8
12 sides	1

Table 2: The number of linear rim segments analyzed with the number of craters displaying them.

**Conclusions:** Our preliminary results show polygonal craters are the most dominant feature seen in our near-global crater database. The number of sides for the polygonal craters is consistent with other findings for Ceres as well as the expected shape of polygonal craters seen throughout the solar system. The most frequent class of polygonal crater is one which shows no effect due to visible fractures, suggesting the influence of subsurface fractures, as theorized for Samhain Catenae [10]. Future work includes (1) identifying the distribution of these features and (2) comparing these data to the morphometric information acquired for the central peaks and central pits. Results of this work will provide additional insight into the evolution and nature of the crust of Ceres.

**Acknowledgements:** This research is supported by NASA PGG award NNX14AN27G to NGB.

**References:** [1] Öhman T. (2009) *The Structural Control of Polygonal Impact Craters*, 15-177. [2] Kopal Z. (1966) *An Introduction to the Study of the Moon*, 266-297. [3] Singer K.M. and McKinnon W.B. (2011) *Icarus*, 216, 198-211. [4] Öhman T. et al. (2008) *Meteoritics & Planetary Science*, 43, 1605-1628. [5] Öhman T. et al. (2006) *Meteoritics & Planetary Science*, 41, 1163-1173. [6] Neidhart T. et al. (2017), *48<sup>th</sup> LPSC*, 1625. [7] Otto K. A. et al. (2016) *47<sup>th</sup> LPSC*, 1493. [8] Gou S. et al. (2018) *Icarus*, 302, 296-307. [9] Rotasch T. et al. (2017) *Planet. Space Sci.*, 140, 74-79. [10] Scully J. E. C. et al. (2017), *GRL*, 44, 9564-9572.